

Dielectric Constant, Loss Tangent, and Surface Resistance of PCB Materials at K -Band Frequencies

Victor N. Egorov, Vladimir L. Masalov, Yuri A. Nefyodov, Artem F. Shevchun, Mikhail R. Trunin, Victor E. Zhitomirsky, and Mick McLean

Abstract—This paper develops the theoretical approach and describes the design of a practical test rig for measuring the microwave parameters of unclad and laminated dielectric substrates. The test rig is based on a sapphire whispering-gallery resonator and allows the measurement of the following parameters: dielectric constant (ϵ) of the dielectric substrate in the range from 2 to 10, loss tangent ($\tan \delta$) of the dielectric substrate in the range from 10^{-4} to 10^{-2} , and microwave losses of copper coating of the substrate in the range from 0.03 to 0.3 Ω . Measurements of numerous commonly used microwave printed-circuit-board materials were performed at frequencies between 30–40 GHz and over a temperature range of -50 °C to $+70$ °C.

Index Terms—Anisotropy, complex permittivity, dielectric resonator (DR), resonance spectrum, surface resistance, whispering-gallery (WG) modes.

I. INTRODUCTION

ESSENTIAL parameters needed for the efficient design of integrated microwave circuits are dielectric properties (ϵ and $\tan \delta$), the degree of passive intermodulation, and the microwave copper resistance of the printed-circuit-board (PCB) substrate on which the active elements are mounted. As components are increasingly miniaturized and frequencies increased, the need for accurate dielectric measurements of low-loss substrate materials increases. The properties of these materials should be known over a wide temperature range.

Resonant measurement methods represent the most accurate way of obtaining the dielectric constant and loss tangent with unclad thin materials [1], [2]. The high value of the unloaded quality factor Q_0 of the resonator enables measurements of the smallest losses in the test materials. Methods based on bulk resonators have been developed in numerous laboratories and the results widely published [1]–[5]. The cylindrical TE_{01p} cavity

has been used to measure both the in-plane dielectric parameters for thin dielectric samples and surface resistance [6]–[8]. However, at room temperature, the Q_0 of bulk resonators does not exceed 10^4 in the millimeter-wavelength band. The open hemispherical resonator [3], [4], [9] is a very sensitive instrument for in-plane dielectric measurements of very low loss and flat specimens with diameters much greater than the wavelength. There are two problems with this approach: nonflatness of real samples and large resonator sizes, which limit the application of this technique for measurements in a wide temperature range. Microstrip-based tests [10] do not allow the dielectric and ohmic losses to be measured separately. The nonreproducibility of the rig connection impedance limits the accuracy of this method. A cylindrical TE_{016} dielectric split resonator [11] made from thermally stable high-permittivity ceramic has been successfully used for in-plane dielectric film measurements at frequencies below 10 GHz, but it was found unsuitable for measurements at higher frequencies due to increased loss tangent in ceramic materials and, hence, decrease of Q_0 .

In all the above-mentioned methods, the interface surface of the specimen is placed along the microwave E -field. At the same time, most PCBs operate with the electric field primarily normal to the plane of the sheet. An incident electromagnetic field should, therefore, have an electric-field component orthogonal to the sample surface. The sapphire disk “whispering gallery” (WG) resonator [12] has Q_0 at approximately 40 000 at room temperature in the range of 40 GHz (wavelength λ of approximately 8 mm) and a typical diameter approximately 1.5λ . There are two WG-mode types: quasi- E (or HE) and quasi- H (or EH) with a high Q_0 value for a large azimuth mode index $n \gg 1$. They can be used for dielectric substrate measurements with orthogonal and tangential microwave E -fields, respectively. A significant and universal problem with making dielectric measurements with an orthogonal field is the so-called “residual air-gap,” which exists due to the microroughness at the contact between the flat resonator and specimen surfaces. As a result, an effective “residual air gap” should be taken into consideration in the electrodynamic model of the measured structure.

The goal of this paper is to evaluate both theoretically and experimentally the uncertainties of the sapphire disk WG dielectric-resonator (DR) technique for measurements of out-of-plane dielectric properties of thin materials using up to five different resonance HE_{n11} modes. Acceptable accuracy of measurement

Manuscript received January 5, 2004; revised February 16, 2004. This work was supported by the National Measurement System Directorate of the U.K. Department of Trade and Industry. The work of Y. A. Nefyodov was supported by the Russian Science Support Foundation.

V. N. Egorov and V. L. Masalov are with the East-Siberian Research Institute of Physico-Technical and Radioengineering Measurements, Irkutsk 664056, Russia (e-mail: egorov@irk.ru; masalov@niftri.irkutsk.ru).

Y. A. Nefyodov, A. F. Shevchun, and M. R. Trunin are with the Institute of Solid-State Physics, Russian Academy of Sciences, Chernogolovka, Moscow 142432, Russia (e-mail: nefyodov@issp.ac.ru; shevchun@issp.ac.ru; trunin@issp.ac.ru).

V. E. Zhitomirsky and M. McLean are with Scientific Generics, Cambridge GB2 5GG, U.K. (e-mail: Victor.Zhitomirsky@genericsgroup.com; Mick.McLean@genericsgroup.com).

Digital Object Identifier 10.1109/TMTT.2004.841219

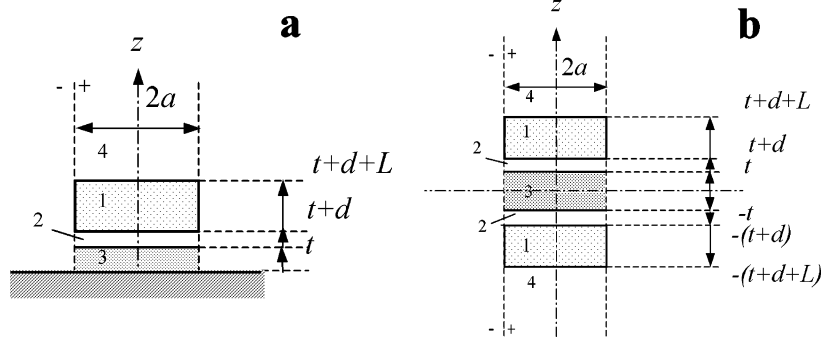


Fig. 1. (a) DR 1 above a metallic plane with dielectric layer 3 inserted in between, the residual air gap 2 is also shown. (b) Dielectric layer in the split DR.

was provided for both extremely thin substrates with a thickness down to $30 \mu\text{m}$, as well as for very thick substrates with a thickness exceeding 1 mm . This is possible because the DR achieves a substantial filling factor value even with very thin substrates. A high- Q factor of the DR also helps to accurately measure very small changes to the resonance frequency. An accuracy of 1% for permittivity measurements of thin dielectric materials and a resolution of the order of 10^{-4} for their loss tangent has been shown at 40 GHz. Our test method also allows the measurement of the effective microwave surface resistance of laminated metal at the interface between the laminated material and dielectric.

II. ELECTRODYNAMICS

A. Measurement Structure Basic

Below we describe the resonance mode structure of a dielectric cylinder [see Fig. 1(a)] with diameter $2a$ and height L , which is separated from a metallic plane by a dielectric layer of height t and a gap of height d . If the component of the electric field in the z -direction $E_z(z)$ is an even function of z , then the plane $z = 0$ (metallic surface) behaves as a so-called “electric wall” for which the following boundary conditions are satisfied: $E_{3r} = E_{3\varphi} = 0$. The electrodynamic structure of the modes in such a case is equivalent to the modes of the split DR with a dielectric layer of double height $2t$ in the slot [see Fig. 1(b)].

The relative permittivity of a DR is characterized by a tensor

$$\hat{\epsilon}_1 = \begin{pmatrix} \epsilon_{1\perp} & 0 & 0 \\ 0 & \epsilon_{1\perp} & 0 \\ 0 & 0 & \epsilon_{1\parallel} \end{pmatrix}$$

which determines its electric properties, and by a scalar μ_1 for the magnetic properties. Symbols \parallel and \perp are related to the components of $\hat{\epsilon}_1$ in the direction along the optical (geometrical) axis and in the plane perpendicular to this axis, respectively. We use ϵ_3, μ_3 for the isotropic dielectric layer, and ϵ_2, μ_2 for the ambient isotropic space, which includes both the top space 4 and gap 2. We analyze the electromagnetic resonance modes by the method of approximate separation of variables with one-mode approximation of the fields at all fractional volumes of the resonator [9]. In this approach, an electromagnetic field at frequency ω inside the resonator within the boundaries $t + d \leq$

$z \leq t + d + L$ is represented in the form of linear combination of standing E - and H -waves, which forms a hybrid standing HE or EH wave along the z -axis. Transverse (on r, φ coordinates) field distribution in gap 2, the dielectric layer 3 and top space 4 is assumed the same as in disk 1. The longitudinal wavenumbers h_{1E} and h_{1H} of the E - and H -waves, respectively, are the same and are equal to the longitudinal wavenumber of the hybrid wave in disk 1: $h_{1E} = h_{1H} = h$. The boundary conditions $E_{1\varphi}^+ = E_{1\varphi}^-$, $H_{1\varphi}^+ = H_{1\varphi}^-$ for inside (+) and outside (-) field components at $r = a$ within the limits $t + d \leq z \leq t + d + L$ ($i = 1$) define the equation of a circular “dielectric post resonator” with single axis anisotropy [13]

$$\begin{aligned} & \left[\frac{\epsilon_{\parallel} J_n'(\alpha\chi_1 a)}{\alpha\chi_1 a J_n(\alpha\chi_1 a)} - \frac{H_n^{(2)'}(\chi_2 a)}{\chi_2 a H_n^{(2)}(\chi_2 a)} \right] \\ & \times \left[\frac{\mu J_n'(\chi_1 a)}{\chi_1 a J_n(\chi_1 a)} - \frac{H_n^{(2)'}(\chi_2 a)}{\chi_2 a H_n^{(2)}(\chi_2 a)} \right] \\ & - \left(\frac{nh}{k_2} [(\chi_1 a)^{-2} - (\chi_2 a)^{-2}] \right)^2 = 0 \end{aligned} \quad (1)$$

where $J_n(\chi_1 a)$, $H_n^{(2)}(\chi_2 a)$, $J_n'(\chi_1 a)$, and $H_n^{(2)'}(\chi_2 a)$ are the Bessel and Hankel functions of the order n and their derivatives, χ_1 and χ_2 are the inside (+) and outside (-) transverse wavenumbers, respectively, $\epsilon_{\parallel} = \epsilon_{1\parallel}/\epsilon_2$, $\mu = \mu_1/\mu_2$, and $\alpha = \sqrt{\epsilon_{1\parallel}/\epsilon_{1\perp}}$. For $\epsilon_{\parallel} = \epsilon_{\perp} \equiv \epsilon_{1\perp}/\epsilon_2$, this equation is reduced into the equation of an isotropic “dielectric post resonator” [14], [15].

For HE_{nmp} modes with odd longitudinal index $p = 2q + 1$ ($q = 0, 1, 2, \dots$), the boundary conditions at $z = 0$, $z = t$, $z = t + d$, and $z = t + d + L$ result in the characteristic equation [13]

$$\begin{aligned} hL - a \tan \frac{h_{2E}\eta_{1E}}{h} \\ - a \tan \left(\frac{h_{2E}\eta_{1E}}{h} \tanh \left(a \tanh \times \left(\frac{h_{3E}}{h_{2E}\eta_{3E}} \tanh(h_{3E}t) \right) \right. \right. \\ \left. \left. + h_{2E}d \right) \right) - (p-1)\pi = 0 \end{aligned} \quad (2)$$

where $\eta_{1E} = \varepsilon_{1\perp}/\varepsilon_2$, $\eta_{3E} = \varepsilon_3/\varepsilon_2$, and h_{iE} are the longitudinal wavenumbers in regions $i = 2, 3, 4$ (Fig. 1)

$$\begin{aligned} h &= \sqrt{k_1^2 - \chi_1^2} = \sqrt{k_2^2 - \chi_2^2} \\ h_{2E} &= \sqrt{(\alpha\chi_1)^2 - k_2^2} \\ h_{2E} &= h_{4E} \\ h_{3E} &= \sqrt{(\alpha\chi_1)^2 - k_3^2} \\ k_1 &= k_0\sqrt{\varepsilon_{1\perp}\mu_1} \\ k_2 &= k_0\sqrt{\varepsilon_2\mu_2} \\ k_3 &= k_0\sqrt{\varepsilon_3\mu_3} \\ k_0 &= \omega\sqrt{\varepsilon_0\mu_0}. \end{aligned}$$

The set of (1) and (2) defines the values h , χ_1 , and $k_1 = \sqrt{h^2 + \chi_1^2}$, which depend on the relative dielectric sample permittivity $\varepsilon = \varepsilon_3/\varepsilon_2$. Equation (1) does not explicitly depend on ε and for determination of ε , one should solve (1) and (2) in series with the values of k_1 and k_2 at the measured resonant frequencies.

The electrodynamic model described by (1) and (2) does not take into account an influence of the part of the dielectric sample at $r > a$, $0 \leq |z| \leq t$, i.e., outside the resonator. If this sample volume is taken properly into account, the resonant frequencies will decrease and, hence, (1) and (2) (which do not take this into account) will overestimate values for ε . The dielectric sample volume outside the resonator is exposed to only a small part of the total electromagnetic energy. This enables one to correct the value of the dielectric constant by the perturbation method

$$\varepsilon_{\text{corr}} = \varepsilon \cdot [1 - (\varepsilon - 1)K_{2E}] \quad (3)$$

where $K_{2E} = W_2^E/W_\Sigma = -2(\varepsilon_2/\omega)(\partial\varepsilon_2/\partial\omega)^{-1}$ and W_Σ , W_2^E are the total resonator energy and electric field energy outside the resonator disks. Factor K_{2E} can be found by numerical differentiation of (1) and (2) with respect to the ambient media permittivity ε_2 [16]. K_{2E} is of the order of 0.01–0.02.

B. Dielectric Permittivity and Loss-Tangent Measurements of Nonmetallic Substrates

For measurements of the dielectric permittivity and loss tangent of the substrate, the foil is removed from both sides of the microwave PCB sample. The sample (substrate) is clamped between the plates of the split DR [see Figs. 1(b) and 2(a)]. In the experiment, the values of the resonant frequencies of HE_{n11} modes are determined. The basic data for calculating the dielectric permittivity of the sample using (1) and (2) are: 1) resonant frequency f_n of HE_{n11} modes with known azimuth index n ; 2) dimensions a and L of the DR; 3) sapphire dielectric permittivities $\varepsilon_{1\parallel}$, $\varepsilon_{1\perp}$; and 4) the thickness t of the sample. The value of a residual air-gap d is determined by the roughness of the surfaces of both the measured sample and the faces of the resonator and cannot be measured directly. One can estimate this value from the condition that the measured value ε_3 should not be dependent on the frequency of the measurements in a narrow frequency interval, which is defined by the frequencies of neighboring (by azimuth index) $HE_{n-1,1,1}$, $HE_{n,1,1}$,

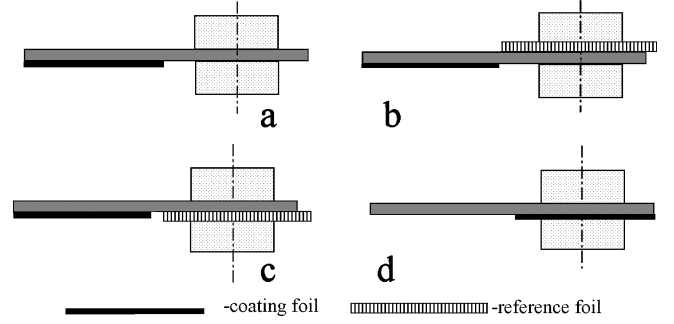


Fig. 2. Schemes for measurements of: (a) ε , $\tan \delta$, (b) $R_{S\text{ref}}$, (c) Q_{ref} , and (d) q_σ , R_s .

and $HE_{n+1,1,1}$ resonance modes. The frequency dispersion of low-loss dielectric samples in such a narrow frequency range is usually negligible in comparison with the uncertainty of the real measurements. The problem of the unknown residual air gap makes an additional contribution to inaccuracy, which slightly reduces the measured value ε_3 . Uncertainty of the measurements depends on the frequency and is reduced with the increase of the azimuth index n of the resonant mode.

The electromagnetic power $P_{\delta 3}$ directly absorbed by the sample [dielectric layer 3 in Fig. 1(b)] and electromagnetic energy W_3^E stored in the sample layer are connected by the relationship $P_{\delta 3} = \omega W_3^E \tan \delta$, where δ is the dielectric loss angle of a measured sample. In the ordinary approximation of the additive contribution of different losses, the power $P_{\delta 3}$ is connected with the total power loss P_Σ and the unloaded quality factor $Q_{0\Sigma}$ of the resonator by the following equation:

$$\begin{aligned} \frac{1}{Q_{0\Sigma}} &= \frac{P_\Sigma}{\omega W_\Sigma} \\ &= \frac{P_{\delta 1} + P_{\delta 3} + P_{\text{rad}}}{\omega W_\Sigma} \\ &= \frac{1}{Q_{0\text{DR}}} + \frac{W_3^E}{W_\Sigma} \tan \delta + \frac{1}{Q_{\text{rad}}} \end{aligned} \quad (4)$$

where $P_{\delta 1}$ is a dielectric loss power in the resonator dielectric disks only, $Q_{0\text{DR}}$ is a partial quality factor of these disks, P_{rad} is the radiant loss, and Q_{rad} is the radiant quality factor of the resonator. It is easy to satisfy the condition $Q_{0\text{DR}}^{-1} + W_3^E \cdot \tan \delta / W_\Sigma \gg Q_{\text{rad}}^{-1}$ by choosing dimensions of the DR. In this case, from (4), we get

$$\tan \delta = K_{3E}^{-1} (Q_{0\Sigma}^{-1} - Q_{0\text{DR}}^{-1}) \quad (5)$$

where $K_{3E} = W_3^E/W_\Sigma$ is a filling factor of the resonator. The value of K_{3E} can be obtained from the value of the stored energy by integrating the field components over the corresponding volumes of the resonator

$$\begin{aligned} W_i^E &= \frac{\varepsilon_0 \varepsilon_i}{2} \int_{V_i} |\vec{E}|^2 dV \\ W_\Sigma &= \sum_i W_i^E = \sum_i W_i^H, \quad i = 1, 2, 3, 4 \end{aligned} \quad (6)$$

where $W_i^{E,H}$ is the energy of the electric or magnetic field stored in the V_i -volume of the resonator. Another way to calculate K_{3E} is by numerical differentiation of the $\varepsilon_3(\omega)$ function

obtained from (1) and (2) at measured resonant frequencies ω of the resonator with a sample inside [16]

$$K_{3E} = -2 \frac{\varepsilon_3}{\omega} \left(\frac{\partial \varepsilon_3}{\omega} \right)^{-1}. \quad (7)$$

The quantity Q_{0DR} in (5) is the unloaded quality factor of the resonator with a hypothetical sample, which has the dielectric permittivity of the real sample, but has no loss ($\tan \delta = 0$). The value Q_{0DR} is close to the unloaded Q_{00} of the split resonator without a sample and can be found from the equation

$$Q_{0DR}^{-1} = K_{1\parallel} \cdot \tan \delta_{\parallel} + K_{1\perp} \cdot \tan \delta_{\perp} \quad (8)$$

where $K_{1\parallel} = W_{1\parallel}^E / W_{\Sigma}$, $K_{1\perp} = W_{1\perp}^E / W_{\Sigma}$, and $W_{1\parallel}^E + W_{1\perp}^E = W_{\Sigma}^E$. Here, $W_{1\parallel}^E$ and $W_{1\perp}^E$ are the energy stored in the longitudinal and transverse components of electric field \vec{E} in the sapphire disks with a sample between them; $\tan \delta_{\parallel}$ and $\tan \delta_{\perp}$ are the components of the loss tangent tensor of sapphire in the direction of optic axis and in the plane perpendicular to this axis, respectively.

Similarly to (6) and (7), the coefficients $K_{1\parallel}$ and $K_{1\perp}$ are calculated via integration of longitudinal and transverse components of vector \vec{E} or by numerical differentiation of the resonant frequency dependences

$$K_{1\parallel} = -2 \frac{\varepsilon_{1\parallel}}{\omega} \left(\frac{\partial \omega}{\partial \varepsilon_{1\parallel}} \right) \quad K_{1\perp} = -2 \frac{\varepsilon_{1\perp}}{\omega} \left(\frac{\partial \omega}{\partial \varepsilon_{1\perp}} \right). \quad (9)$$

C. Surface-Resistance Measurements Under Dielectric

To measure the surface resistance R_S of the metallic foil on its interface with the dielectric material, disk 1 is pressed against unclad surface of the sample [see Figs. 1(a) and 2(d)]. In order to determine R_S , we will use values of the filling factor K_{3E} for the laminated sample and the unloaded quality factor Q_{0DR} of the resonator, as well as $\tan \delta$ of an unclad sample measured in accordance with the procedure described in Section II-B. Similarly to (4) and taking into account (5), the unloaded quality factor $Q_{0\Sigma\sigma}$ of the resonator pressed onto the dielectric sample with a copper laminated layer is defined as

$$\frac{1}{Q_{0\Sigma\sigma}} = \frac{P_{\Sigma\sigma}}{\omega W_{\Sigma}} = \frac{1}{Q_{0DR}} + K_{3E} \cdot \tan \delta + \frac{1}{Q_{\sigma}} \quad (10)$$

where $P_{\Sigma\sigma}$ is the total loss power, $Q_{\sigma} = \omega W_{\Sigma} / P_{\sigma}$ is a partial Q factor due to ohmic loss in the metallic foil, and P_{σ} is an ohmic loss power, which is equal to

$$P_{\sigma} = R_S \int_S |H_{\tau}|^2 \frac{dS}{2} \quad (11)$$

where H_{τ} is the tangential component of the microwave magnetic field on the surface of the metal; S is the surface area at the interface between the metallic foil and the dielectric layer. Total energy W_{Σ} stored in the resonator can be found by integrating the magnetic-field energy in partial resonator volumes

$$W_{\Sigma} = \sum_i W_i^H \quad W_i^H = \frac{\mu_0 \mu_i}{2} \int_{V_i} (|H_{i\perp}|^2 + |H_{iz}|^2) dV. \quad (12)$$

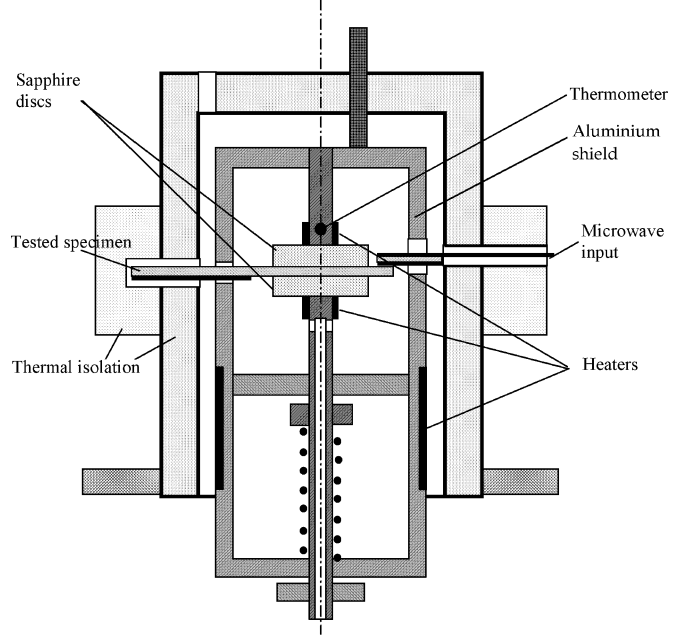


Fig. 3. Measurement cell diagram.

From (10)–(12), we get the surface resistance of the laminated dielectric sample

$$R_S = \frac{\pi f_n \mu_0 M}{Q_{\sigma}} \quad (13)$$

where $Q_{\sigma}^{-1} = Q_{0\Sigma\sigma}^{-1} - Q_{0DR}^{-1} - K_{3E} \cdot \tan \delta$. Neglecting the contribution of the longitudinal component of the magnetic field in (12), a geometric factor M is calculated in [17].

III. EXPERIMENT

A. Measurement Cell

A simplified schematic of the measurement cell is shown in Fig. 3. A sample is placed between polished sapphire disks with diameter of 12.51 mm and a height of 2.54 mm, which are arranged inside a thick-wall aluminum shield with an inner diameter of 25 mm. The diameter of the shield was chosen to exclude any influence of the metal wall on either the resonant frequencies or the quality factors of the sapphire disks. The aluminum shield is placed inside a thermal isolation chamber. The lower sapphire disk is attached to the post guide and clamped to the sample through the spring with the pressure of approximately three bars.

We took special care to prepare “nearly ideal” DRs. Sapphire disks were cut from the same piece of a carefully oriented sapphire single crystal of very high chemical purity. The dimensions of both disks were identical to an accuracy of within $1 \mu\text{m}$. The c -axis of both the disks was perpendicular to their faces. The faces of each disk were parallel with the accuracy better than $1 \mu\text{m}$ across the disks diameter. Surface roughness reduced to 2 nm after polishing. The deviation from flatness of each surface was less than $0.5 \mu\text{m}$ across each disk’s diameter. As a result, the problem of the “residual air-gap” was significantly reduced even when the two disks were brought into contact without a “soft” dielectric film between them. Moreover, because these two disks

in close mechanical contact constitute a near-perfect monolithic crystal, no measurable splitting of the resonance curves has been detected.

To simplify the process of changing dielectric samples, the post guide is designed to be axially moveable and have no radial free play. The aluminum shield with sapphire disks and sample can be moved toward and away from the microwave microstrip line by a stepper motor (not shown) in order to tune the coupling of the transmission line with the DR. The latter was included into the line as a directional coupler. Coupling change had not resulted in the resonance frequency shift. Semirigid coaxial cables connect the microstrip to standard 2.9-mm connectors outside the cell thermal isolation. The measuring cell is placed in a stainless-steel vacuum cryostat with a temperature control system. For low-temperature measurements, liquid nitrogen is evaporated from the cryostat and its vapor flows around the resonator and the aluminum shield. Rhode&Schwarz SMR-40 and Gigatronics-8541C were used as the generator and power meter, respectively.

B. Experimental Procedure and Results

The procedure for taking measurements of dielectric constant, loss tangent, and surface resistance of one-side laminated dielectric samples is described below.

First, the resonant spectrum (resonator output microwave power P versus frequency f) of the upper DR is measured. For this measurement, the lower resonator is moved away by a maximum distance of 3 mm from the upper resonator and does not influence the measured quantities. Thereupon we determine the resonant frequencies f_n , loaded quality factors Q_{Ln} , and coupling coefficients β_n of HE_{n11} modes ($8 \leq n \leq 12$) of the upper resonator in the range $30 \leq f_n \leq 40$ GHz. At room temperature $T = 22$ °C, the unloaded quality factors $Q_n = Q_{Ln}(1 + \beta_n)$ of the HE_{n11} modes with $n = 8, 9, 10, 11, 12$ are equal to 35 790, 40 850, 45 360, 44 970, 37 080, respectively. The maximum quality factor corresponds to the $HE_{10,1,1}$ mode. The further increase of azimuth index n results in a drop in Q_n due to the increase of the sapphire loss tangent. The measured values of resonant frequencies and quality factors for HE_{n11} modes of the single resonator at different temperatures within the range $-50 \leq T \leq 70$ °C are saved into computer memory as calibration constants.

We proceed with similar measurements with both sapphire disks pressed together and determine the values of resonant frequencies and quality factors for HE_{n11} modes of this doubled resonator at the same temperatures $-50 \leq T \leq 70$ °C. The results obtained are also stored into the computer memory for further calculations of the dielectric constant, loss tangent, and surface resistance of laminated dielectric samples.

The measured frequencies f_n^2 of the double resonator are significantly lower than corresponding frequencies f_n^1 of the single one. The difference $(f_n^1 - f_n^2)$ decreases when the azimuth number n increases. For example, it is equal to 4406 MHz for $n = 9$ and 3637 MHz for $n = 12$. This approximately corresponds to the theoretical calculations for the double resonator. Results of theoretical calculations using (1) and (2) are shown in Table I along with the measured resonant frequencies. In these calculations, we used sapphire permittivities of $\varepsilon_{1||} = 11.577$

TABLE I
RESONANT FREQUENCIES OF HE_{n11} MODES

n	Single resonator			Doubled resonator		
	f_{calc} , GHz	f_n^1 , GHz	$\delta f \cdot 10^2$	f_{calc} , GHz	f_n^2 , GHz	$\delta f \cdot 10^2$
9	32.9767	33.3873	-1.23	28.8439	28.9808	-0.47
10	35.1495	35.4969	-0.98	31.2617	31.3881	-0.40
11	37.3448	37.6594	-0.84	33.6768	33.7958	-0.35
12	39.5590	39.8415	-0.71	36.0889	36.2041	-0.32

and $\varepsilon_{1\perp} = 9.388$ [18]. The discrepancy $\delta f = (f_{calc} - f_n)/f_n$ between the calculated f_{calc} and measured f_n frequency values does not exceed 1.3% for the single resonator and 0.5% for the doubled resonator.

Dielectric sheet samples used for measurements of the dielectric constant and loss tangent have planar dimensions 25×50 mm², thickness up to 1 mm, and a one-side copper-laminated square surface of 25×25 mm². The sample is held with force between the upper and lower resonators [see Fig. 2(a)] providing the sapphire disks are in the center of the square 25×25 mm² surface. When the sample is clamped inside the split DR, the measured resonant frequencies $f_{n\varepsilon}$ are shifted down compared to the frequencies f_n of the single resonator. The problem of identification of the $HE_{n,1,1}$ mode arises. Fortunately, however, first the coupling of the $HE_{n,1,1}$ modes are the highest, and secondly, the frequency difference $\Delta f = f_{n,\varepsilon} - f_{n-1,\varepsilon}$ between the nearest $HE_{n,1,1}$ and $HE_{n-1,1,1}$ modes is almost independent for $n \geq 9$.

If the mode identification was correct, the results of calculations for all the modes give very close values for both the permittivity and loss tangent. The mean values of ε and $\tan \delta$ are calculated using results obtained for all modes. The results are weighted according to the uncertainty of the resonance curve fitting. Examples of such results obtained for a set of samples at room temperature are shown in Table II. Below mean values, the coefficients $C_\varepsilon = (\partial\varepsilon/(\varepsilon \cdot \partial t)) \cdot 1000$ and $C_\delta = (\partial(\tan \delta)/(\tan \delta \cdot \partial t)) \cdot 1000$ are shown. These values are introduced as correction coefficients describing the influence of the absolute uncertainty Δt (in micrometers) in measurements of the thickness of the sample. The error for permittivity can then be found by the formula $\Delta\varepsilon/\varepsilon = C_\varepsilon \cdot \Delta t/1000$. Similarly, the error in the loss tangent value is given by $\Delta(\tan \delta)/\tan \delta = C_\delta \cdot \Delta t/1000$.

The test rig allows measurements at different temperatures. Such measurements are made in a similar fashion to those at room temperature. The only difference is that preliminary calibration of the resonance frequencies and quality factors of the single and double resonator are performed in the range of temperatures. The temperature is stabilized at exactly the same values for measurements with and without the sample, which helps to compensate almost completely for the temperature dependence of sapphire dielectric properties. An example of ε and $\tan \delta$ temperature dependences obtained by this scheme for two samples (NY9220 \times 0.01 in and Tly5a0200) is presented in Figs. 4 and 5, respectively.

The method of surface resistance R_S measurements of the laminated dielectric samples is illustrated in Fig. 2(b)–(d). Two approaches are possible here, which are: (I) direct measurements and (II) measurements using a calibrated reference copper foil. Let us consider them separately.

TABLE II
SAMPLES PARAMETERS AT ROOM TEMPERATURE

SAMPLES		SAMPLES PARAMETERS															
MANUFACTURER'S INFO		AVERAGE VALUES								VALUES FOR PARTICULAR MODE (9-12)							
Sample/Company Material	Thick-ness, μm	ϵ (low frequency)	$\epsilon \pm \Delta\epsilon$	$\tan\delta \times 10^3$	$\pm\Delta\tan\delta \times 10^3$	R_s , Ohm	$\pm\Delta R_s$, Ohm	f_{diel} , GHz	Q_{diel}	Uncer-tainty, %	ϵ	$\tan\delta \times 10^3$	$f_{\text{metal+diel}}$, GHz	$Q_{\text{metal+diel}}$	Uncer-tainty, %	R_s , Ohm	
RO3003x0.01"/ Rogers PTFE ceramic 3.0 / 1.3	255	2.92	2.85	0.03	1.3	0.1	0.24	0.14	31.045	9020	4.8	2.80	0.77	31.733	2806	5.4	0.38
			33.499	6833	4.0	2.84	1.28	34.159	4584	2.9	0.24						
			35.949	7812	1.2	2.85	1.27	36.551	5986	5.8	0.22						
			38.375	8565	8.3	2.85	1.28	38.916	6694	14.1	0.28						
RO3003x0.03"/ Rogers PTFE ceramic 3.0 / 1.3	760	2.94	2.93	0.02	1.7	0.3	0.09	+0.1	32.035	4401	13.8	2.97	2.16	32.513	3242	5.4	0.18
			34.418	6394	4.5	2.93	1.84	34.800	4219	6.1	0.10						
			36.759	8054	4.1	2.93	1.76	37.075	5755	0.6	0.06						
			39.080	10241	1.0	2.94	1.50	39.344	9229	5.3	0.10						
NY9220x0.03"/ Nelco Woven PTFE 2.2 / 1.3	755	2.23	2.09	0.02	0.98	0.14	0.110	0.016	32.478	11512	0.7	2.09	0.98	32.833	7720	10.9	0.12
			34.768	13334	7.7	2.09	1.08	35.067	11570	1.4	0.11						
			37.053	16623	3.2	2.09	1.01	37.297	14484	7.1	0.10						
			39.327	18145	3.7	2.09	0.84	39.531	16103	1.7	0.11						
GIG M/L-2/isola	75	3.85	2.90	0.02	7.8	0.7	0.97		29.835	1798	1.5	2.89	7.91	30.268	329	9.4	1.24
			32.314	1829	2.5	2.90	8.10	35.321	71	49.1	0.73						
			34.784	2060	1.7	2.90	7.51	0	0	0	0						
			37.243	1956	5.2	2.92	8.32	0	0	0	0						
NH9348ST0203CHCH/ Neltec PTFE/glass/ceramic 3.48 / 3	205	3.60	3.32	0.03	3.1	1.2	0.36		30.512	2924	2.7	3.32	2.95	31.191	1308	2.3	0.25
			35.499	3270	0.8	3.30	3.27	33.929	1390	11.8	0.15						
			37.949	601	11.1	3.33	21.3	36.111	2566	4.1	0.46						
			0	0	0	0	0	0	0	0	0						
tly5a0200/Taconic PTFE/glass 2.17 / 0.4	525	1.80	2.12	0.02	0.94	0.05	0.09	0.04	32.219	10355	3.5	2.11	0.93	32.700	6228	2.5	0.06
			34.546	12691	2.1	2.13	0.93	34.966	9766	0.7	0.11						
			36.872	14400	2.1	2.13	0.97	37.221	13156	4.7	0.08						
			39.181	16618	2.0	2.13	0.92	39.474	13793	2.5	0.09						
Rogers 5880 PTFE/glass/fiber 2.2 / 0.9	120	2.34	2.16	0.02	0.74	0.25	0.21	0.06	30.632	11703	2.8	2.17	0.63	31.389	4114	3.9	0.18
			33.115	12756	1.5	2.18	0.65	33.848	4579	5.7	0.22						
			35.608	10266	4.4	2.14	0.98	36.274	6067	1.4	0.20						
			38.049	13209	4.3	2.16	0.73	38.673	6463	3.5	0.24						
Sheldahl G2200x2mil	50	1.4	2.99	0.02	12.9	0.9	0.13	0.02	29.561	1442	1.2	2.98	13.1	30.050	922	3.3	0.10
			32.024	1513	4.4	2.98	12.7	32.538	698	1.8	0.14						
			34.481	1547	1.1	2.99	12.8	35.016	932	1.0	0.12						
			36.933	1590	4.5	3.01	12.8	37.479	534	46.4	0.12						
Sheldahl Comclad XFx10mil	280	2.27	2.24	0.02	0.44	0.12	0.07	+0.05	31.518	20103	5.1	2.26	0.24	32.243	10044	4.3	0.10
			33.962	15778	25.6	2.24	0.49	34.598	17829	2.9	0.07						
			36.370	16270	22.0	2.24	0.55	36.924	20839	3.3	0.05						
			38.753	18707	29.1	2.24	0.47	39.235	22934	3.0	0.05						

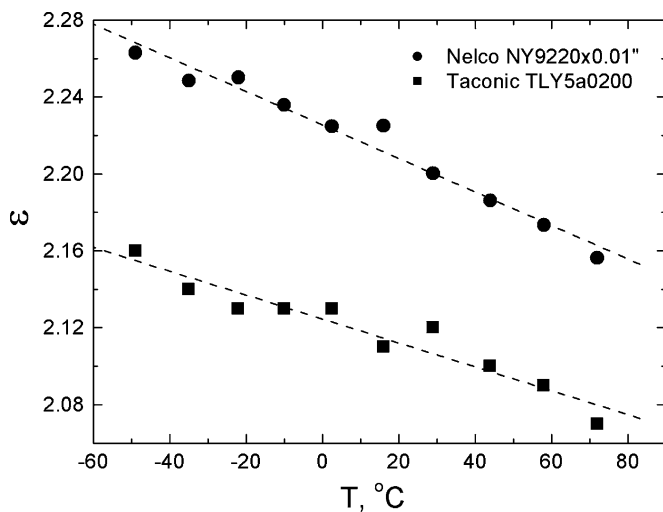


Fig. 4. Temperature dependences of permittivity in NY9220 \times 0.01 in (Nelco) and Tly5a0200 (Taconic).

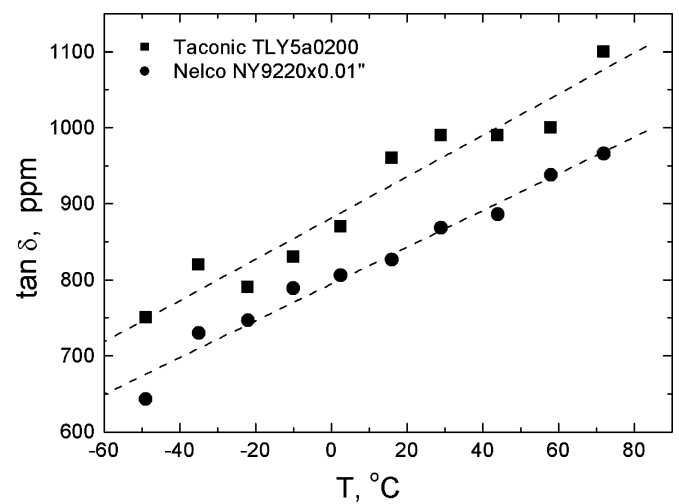


Fig. 5. Temperature dependences of loss tangent in NY9220 \times 0.01 in (Nelco) and Tly5a0200 (Taconic).

(I) The direct method of the surface resistance measurements is based on the calculation of R_s using (13). In this case, the sample is placed into the resonator as shown in Fig. 2(d), and

the quality factor $Q_{0\Sigma\sigma}$ of the upper resonator with laminated dielectric sample is measured. Using the previously determined quality factor Q_{0DR} of the resonator without a sample and the sample loss tangent $\tan\delta$ (obtained by measuring the nonclad

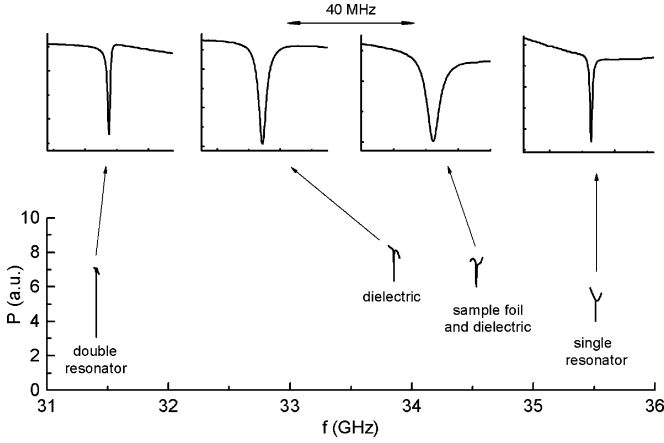


Fig. 6. Evolution of resonance curves of the $HE_{10,1,1}$ mode in the sample RO3003 $\times 0.0''$ (Rogers) for direct measurement of surface resistance.

part of the sample as described above), the value of Q_σ is obtained as follows:

$$Q_\sigma = \left(Q_{0\Sigma\sigma}^{-1} - Q_{0DR}^{-1} - K_{3E} \cdot \tan \delta \right)^{-1} \quad (14)$$

where filling factor K_{3E} is calculated for the laminated sample. Factor Q_σ has appeared before as a denominator in the right-hand side of (13). It characterizes an ohmic loss in the metal lamination at the interface with dielectric material. The geometric factor M is calculated elsewhere [17]. Fig. 6 illustrates the frequency shifts and quality-factor variations for measurements of R_S at the $HE_{10,1,1}$ mode.

The accuracy of the direct surface resistance measurements strongly depends on the thickness t and the dielectric losses in the substrate. To obtain reliable results by this method, ohmic losses in the laminated metal must be comparable to dielectric losses. In case of copper foil, the applicability criteria for direct measurements can be written as $t < 0.1 \cdot (\varepsilon / \tan \delta)$, where the thickness t of the substrate is expressed in μm . In Table II, the R_S data of the fourth, fifth, seventh, eighth, and ninth samples were obtained by direct measurements.

(II) The second method to measure the surface resistance of laminated dielectric samples involves a few extra steps, which are shown in Fig. 2(b)–(d).

Step 1) The smooth copper metal foil is chosen as a reference. The surface resistance of the foil $R_{S\text{ref}}(f)$ (if unknown) is determined by measuring the quality factor of the upper resonator pressed against this foil [see Fig. 2(b)]. Using measurements at the resonance frequencies of several $HE_{n,1,1}$ modes, the surface resistance can be calculated as $R_{S\text{ref}} = \pi f_n \mu_0 M_{\text{ref}} / Q_{\sigma\text{ref}}$, where $Q_{\sigma\text{ref}}^{-1} = Q_{0\Sigma\sigma}^{-1} - Q_{0DR}^{-1}$. The expression for M_{ref} follows from (13) for the resonator located on a metallic plane without dielectric layer ($t = 0$), but with an effective air-gap d . In turn, an effective air gap can be found from (1) and (2), and the condition of equality of double resonator frequency to the frequency of the upper resonator on the metal surface (see [17]).

Step 2) The reference foil is placed underneath the uncoated region of the dielectric sample, and they are held together between the disks of the split resonator [see

Fig. 2(c)]. The quality factors $Q_{0\Sigma\sigma\text{ref}}$ of this sandwich structure are measured for different resonance $HE_{n,1,1}$ modes. The values Q_{ref} at resonant frequencies are found by the following formula:

$$Q_{\text{ref}} = \left(Q_{0\Sigma\sigma\text{ref}}^{-1} - Q_{0DR}^{-1} - K_{3E} \cdot \tan \delta \right)^{-1}. \quad (15)$$

In contrast to $Q_{\sigma\text{ref}}$ determined during the first step, the quality factors Q_{ref} in (15) determine the losses in the reference foil, taking into account the electromagnetic-field distribution in the structure of Fig. 2(c).

Step 3) The same distribution of the field occurs in the geometry shown in Fig. 2(d). The quality factor Q_σ related to the ohmic loss at the interface between the metal foil and the dielectric material is determined in accordance with (14). The surface resistance R_S of the metal foil at the resonant frequencies of the $HE_{n,1,1}$ modes is found as $R_S = R_{S\text{ref}} Q_{\text{ref}} / Q_\sigma$, where the value $R_{S\text{ref}}$ of the reference foil measured at the first step is linearly approximated to the appropriate frequency of the third measurement step.

The advantage of method (II) in comparison with the direct method (I) is that the surface resistance R_S does not depend on the calculation of the geometric factor M in (13) and, hence, the accuracy of method (II) is higher, especially for thicker samples.

IV. CONCLUSION

In this paper, we have presented a novel technique for the measurement of the dielectric constant and loss tangent of dielectric substrates with reasonable accuracy for substrate thickness ranging from 10 to 1000 μm . For the first time, a resonance technique with the electric field of electromagnetic radiation orthogonal to the surface of the substrate has been demonstrated. The high sensitivity for thin samples is made possible by the high unloaded quality factor of the “WG” resonator and substantial filling factor value. There is no fundamental restriction on the maximum thickness of substrate, while its dielectric permittivity is lower than the one of sapphire. When the dielectric thickness increases, the measurement structure shown in Fig. 1 gradually turns to a single DR on the dielectric half-space. Experimental results do not show any influence of the “residual air-gap” problem, which is explained by the optical-quality sapphire polishing, elasticity, and/or flatness of most of the samples, as well as by pressure applied between the sapphire disks and substrate. The method also provides measurements of the surface resistance of metal films. The presence of copper film in the resonator reduces the quality factor by an order of magnitude. The accuracy of surface resistance measurements at the interface between a metallic film and a dielectric layer is strongly influenced by the substrate thickness, dielectric constant, and loss tangent. In the case of $\varepsilon \geq 2$ and $\tan \delta \sim 10^{-4}$, the 15%–20% accuracy of R_S was shown experimentally for dielectric substrate thickness $t \leq 0.2 \div 0.5$ mm. Such materials are widely used at 30–40 GHz.

ACKNOWLEDGMENT

The authors are grateful to S. V. Ryzhkov, V. N. Kurlov, and G. E. Tsydynzhapov, all of the Institute of Solid-State Physics, Russian Academy of Sciences (ISSP RAS), Moscow, Russia, for technical help. The authors would like to thank Rhode&Schwartz, Munich, Germany, for providing the long-term loan of a microwave signal generator. The authors would also like to express their gratitude to the numerous companies that provided samples for their validation measurements. This list includes, but is not limited to Rogers, Chandler, AZ, Labtech, Presteigne, U.K., Spemco, Portsmouth, U.K., Isola, Cumbernauld, U.K., Sheldahl, Nelco, Lannemezan, France, Bookham Technology, Caswell, U.K., and Celestica, Telford, U.K.

REFERENCES

- [1] J. Baker-Jarvis, B. Riddle, and M. D. Janezic, "Dielectric and magnetic properties of printed wiring boards and other substrate materials," NIST, Boulder, CO, Tech. Note 1512, 1999.
- [2] J. Baker-Jarvis, M. D. Janezic, B. Riddle, C. L. Holloway, N. G. Paulter, and J. E. Blendell, "Dielectric and conductor-loss characterization and measurements of electronic packaging materials," NIST, Boulder, CO, NIST Tech. Note 1520, 2001.
- [3] A. L. Cullen and P. K. Yu, "The accurate measurement of permittivity by means of an open resonator," in *Proc. Roy. Soc.*, vol. 325, London, U.K., 1971, pp. 493–509.
- [4] R. J. Cook and R. J. Jones, "Comparison of cavity and open resonator measurements of permittivity and loss angle at 35 GHz," *IEEE Trans. Instrum. Meas.*, vol. IM-23, no. 4, pp. 438–442, Dec. 1974.
- [5] M. N. Afsar and K. J. Button, "Millimeter-wave dielectric measurement of materials," *Proc. IEEE*, vol. 73, no. 1, pp. 131–153, Jan. 1985.
- [6] H. E. Bussey, "Standards and measurements of microwave surface impedance, skin depth, conductivity and Q ," *IEEE Trans. Instrum. Meas.*, vol. IM-9, no. 3, pp. 171–175, Sep. 1960.
- [7] A. Hernandez, E. Martin, and J. M. Zamarro, "Resonant cavities for measuring the surface resistance of metals at X band frequencies," *J. Phys. E., Sci. Instrum.*, vol. 19, pp. 222–225, 1986.
- [8] G. Kent, "Nondestructive permittivity measurement of substrates," *IEEE Trans. Instrum. Meas.*, vol. 45, no. 1, pp. 102–106, Feb. 1996.
- [9] L. A. Vainshtein, *Open Resonators and Open Waveguides* (in Russian). Moscow, Russia: Sov. Radio., 1966.
- [10] *IPC-TM-650 Test Methods Manual*, Inst. Interconnecting and Packaging Electron. Circuits, Northbrook, IL, 1997.
- [11] T. Nishikawa, K. Wakino, H. Tanaka, and Y. Ishikawa, "Precise measurement method for complex permittivity of microwave dielectric substrate," in *Precise Electromagnetic Measurements Conf. Dig.*, Tsukuba, Japan, 1988, pp. 155–156.
- [12] V. F. Vyzjatyshev *et al.*, *A Possibility of Superhigh Quality Resonator Creation* (in Russian). Moscow, Russia: Trudy Moskovskogo Energeticheskogo Instituta, 1978, vol. 360, pp. 51–57.
- [13] V. N. Egorov and I. N. Mal'tseva, "Azimuthal modes in anisotropic dielectric resonator" (in Russian), *Electronnaja Tekhnika. Serija 1, Elektronika SVCH*, no. 2, pp. 36–39, 1984.
- [14] B. W. Hakki and P. D. Coleman, "A dielectric resonator method of inductive capacities in the millimeter range," *IRE Trans. Microw. Theory Tech.*, vol. MTT-9, no. 4, pp. 402–410, Jul. 1960.
- [15] W. E. Courtney, "Analysis and evaluation of a method of measuring the complex permittivity and complex permeability of microwave insulators," *IEEE Trans. Microw. Theory Tech.*, vol. MTT-19, no. 8, pp. 476–485, Aug. 1970.
- [16] V. F. Vyzjatyshev and V. S. Dobromyslov, *The Mutual Correlation of Characteristics in Multilayer Waveguides and Resonators* (in Russian). Moscow, Russia: Trudy Moskovskogo Energeticheskogo Instituta, 1979, vol. 397, pp. 5–7.
- [17] V. N. Egorov, V. L. Masalov, Y. A. Nefyodov, A. F. Shevchun, M. R. Trunin, V. Zhitomirsky, and M. McLean, "Measuring dielectric properties and surface resistance of microwave PCB's in the K -band," [Online]. Available: <http://xxx.lanl.gov/ftp/cond-mat/papers/0312/0312151.pdf>, 2003.
- [18] V. N. Egorov and A. S. Volovikov, "Measuring the dielectric permittivity of sapphire at temperatures 93–343 K," *Radiophys. Quantum Electron.*, vol. 44, no. 11, pp. 885–891, 2001.



Victor N. Egorov was born in Irkutsk, Russia, in 1950. He received the M.Sc. degree in physics and electronics from Irkutsk State University, Irkutsk, Russia, in 1972, and the Ph.D. degree in microwave theory and technique from the Moscow Power Engineering Institute, Moscow, Russia, in 1985.

Since 1975, he has been with the East-Siberian Research Institute of Physico-Technical and Radio-engineering Measurements (VS NIIFTRI), Irkutsk, Russia, where he is currently a Deputy Director. His research interests are mainly concerned with

low-noise microwave generators, high- Q resonators, and microwave parameters measurements.



Vladimir L. Masalov was born in Arkhangel'sk, Russia, in 1941. He received the M.Sc. degree in physics and electronics from the Novosibirsk Electrotechnical Institute, Novosibirsk, Russia, in 1967.

Since 1976, he has been with the East-Siberian Research Institute of Physico-Technical and Radio-engineering Measurements (VS NIIFTRI), Irkutsk, Russia, where he is currently a Senior Researcher. His research interests are mainly concerned with low-noise microwave generators and superconducting resonators and DRs.



Yuri A. Nefyodov was born in Chernogolovka, Russia, in 1977. He received the B.Sc. and M.Sc. degrees in physics and mathematics and Ph.D. degree in condensed matter physics from the Moscow Institute of Physics and Technology (MIPT), Dolgoprudny, Russia, in 1998, 2000, and 2003, respectively.

Since 1997, he has been with the Institute of Solid State Physics, Russian Academy of Sciences (ISSP), Chernogolovka, Moscow, Russia, where he is currently a Researcher. His current research interests are mainly concerned with electro-dynamics

of anisotropic medium, especially with high- T_c superconductors.



Artem F. Shevchun was born in Leipzig, Germany, in 1979. He received the B.Sc. and M.Sc. degrees in physics and mathematics from the Moscow Institute of Physics and Technology (MIPT), Dolgoprudny, Russia, in 2000 and 2002, respectively.

Since 2000, he has been with the Institute of Solid-State Physics (ISSP), Chernogolovka, Moscow, Russia, where he is currently a Junior Researcher. His current research interests are mainly concerned with microwave electro-dynamics of superconductors.



Mikhail R. Trunin was born in Moscow, Russia, in 1958. He received the M.Sc. degree in theoretical physics from Gorky State University, Nizhniy Novgorod, Russia, and the Ph.D. and D.Sc. (habilitation) degrees in condensed matter physics from the Institute of Solid-State Physics (ISSP), Chernogolovka, Moscow, Russia, in 1985 and 1999, respectively.

Since 1980, he has been with the ISSP, where he is a Head of the Laboratory of Electron Kinetics. Since 2000, he has been a Professor with the Moscow Institute of Physics and Technology (MIPT), Dolgoprudny, Russia. His current research interests are concerned with low-temperature physics, superconductivity, and high-frequency electro-dynamics of solids.



Victor E. Zhitomirsky was born in Kharkov, Ukraine, in 1967. He received the B.Sc. and M.Sc. degrees in physics and mathematics and the Ph.D. degree in condensed matter physics from the Moscow Institute of Physics and Technology (MIPT), Dolgoprudny, Russia, in 1987, 1989 and 1993, respectively.

He was a Researcher with the Institute of Solid-State Physics (ISSP). He has held post-doctoral positions with the Max-Planck Institute für Festkörperforschung, Stuttgart, Germany and Oxford University, Oxford, U.K. Since 2001, he has been with the Science and Technology Group, Scientific Generics (SG), Cambridge, U.K., an integrated business and technology consultancy, where he is currently a Senior Consultant. His current research interests are concerned with microwave techniques and disruptive technologies in the area of semiconductors and opto-electronics.



Mick McLean was born in London, U.K., in 1948. He received the B.Sc degree in logic with physics and M.Phil in computer simulation modeling from the University of Sussex, Sussex, U.K., in 1970 and 1979, respectively.

Since joining the Science and Technology Group, Scientific Generics (SG), Cambridge, U.K., a business and technology consultancy group, in 1989, he has managed over 300 assignments involving technology management for private- and public-sector clients. He is also Director and General Manager of

Technical Investment Services Ltd.—the specialist “due diligence” company within the Generics Group launched in January 2001.